Disposition of Docosahexaenoic Acid-Paclitaxel, a Novel Taxane, in Blood: *In Vitro* and Clinical Pharmacokinetic Studies[1]

Alex Sparreboom,[2] Antonio C. Wolff, Jaap Verweij, Yelena Zabelina, Desiree M. van Zomeren, Gregory L. McIntire, Charles S. Swindell, Ross C. Donehower, and Sharyn D. Baker[3]

Department of Medical Oncology, Erasmus MC—Daniel den Hoed Cancer Center, 3075 EA Rotterdam, the Netherlands [A. S., J. V., D. M. v. Z.]; Divisions of Medical Oncology [A. C. W., R. C. D.] and Experimental Therapeutics [Y. Z., S. D. B.], The Sidney Kimmel Comprehensive Cancer Center at Johns Hopkins, Baltimore, Maryland 21231; and Protarga, Inc., King of Prussia, Pennsylvania 19406 [G. L. M., C. S. S.]

ABSTRACT

Purpose: **Docosahexaenoic acid-paclitaxel is as an inert prodrug composed of the natural fatty acid DHA covalently linked to the C2′-position of paclitaxel (M. O. Bradley *et al.*, Clin. Cancer Res., *7:* 3229–3238, 2001). Here, we examined the role of protein binding as a determinant of the pharmacokinetic behavior of DHA-paclitaxel.**

Experimental Design: **The blood distribution of DHA-paclitaxel was studied *in vitro* using equilibrium dialysis and in 23 cancer patients receiving the drug as a 2-h i.v. infusion (dose, 200-1100 mg/m^2).**

Results: In vitro, **DHA-paclitaxel was found to bind extensively to human plasma (99.6 ± 0.057%). The binding was concentration independent ($P = 0.63$), indicating a nonspecific, nonsaturable process. The fraction of unbound paclitaxel increased from 0.052 ± 0.0018 to 0.055 ± 0.0036 (relative increase, 6.25%; $P = 0.011$) with an increase in DHA-paclitaxel concentration (0–1000 μg/ml), suggesting weakly competitive drug displacement from protein-binding sites. The mean (± SD) area under the curve of unbound paclitaxel increased nonlinearly with dose from 0.089 ± 0.029 μg·h/ml (at 660 mg/m^2) to 0.624 ± 0.216 μg·h/ml (at 1100 mg/m^2), and was associated with the dose-limiting neutropenia in a maximum-effect model ($R^2 = 0.624$). A comparative analysis indicates that exposure to Cremophor EL and unbound paclitaxel after DHA-paclitaxel (at 1100 mg/m^2) is similar to that achieved with paclitaxel on clinically relevant dose schedules.**

Conclusions: **Extensive binding to plasma proteins may explain, in part, the unique pharmacokinetic profile of DHA-paclitaxel described previously with a small volume of distribution (~4 liters) and slow systemic clearance (~0.11 liters/h).**

INTRODUCTION

Paclitaxel belongs to the class of taxane diterpenoids (taxoids), and contains a C-20 carbon skeleton derived biogenetically from geranylgeranyol PP_i with a unique tricyclopentadecane ring system as the core structure. The compound is highly lipophilic, virtually insoluble in water (<0.010 mg/ml), and is currently formulated for clinical use in a mixed solvent system containing purified polyoxyethylated castor oil (CrEL)[4] and 49.7% (v/v) dehydrated ethanol, USP (1). To increase aqueous solubility, the design and synthetic preparation of numerous paclitaxel analogues have been described (2). A prodrug approach would be ideal for this situation, because spontaneous hydrolysis or enzymatic cleavage of the analogue converts it back to paclitaxel, and would thus retain the pharmacological activity associated with the parent drug. Structure-activity relationships have shown that the hydroxyl moiety at C-2′, which is essential for cytotoxic activity and tubulin polymerization, offers the preferred handle for the synthesis of inert prodrugs (3).

In addition to solving solubility issues, linkage of specific carriers to paclitaxel offers the possibility of targeted drug delivery that may enhance the therapeutic index (4). The potential targeting of paclitaxel to tumor cells has been investigated with the use of enzyme-activatable prodrugs (5–7) or receptor-mediated-based approaches (8, 9). Studies have demonstrated tumoral uptake of some ω-3 fatty acids from arterial blood (10). DHA-paclitaxel (Fig. 1), a 2′-acyl derivative of the natural fatty acid DHA and paclitaxel, was shown to be associated with significantly enhanced tumor distribution and antitumor activity in various tumor models as compared with paclitaxel after equitoxic or equimolar doses (11). The clinical preparation of the prodrug (*i.e.*, Taxoprexin Injection) is administered as a 2-h infusion in a vehicle that contains 81% less CrEL than Taxol on a molar basis. In a Phase I study, the disposition of DHA-

Received 5/17/02; revised 8/7/02; accepted 8/20/02.

The costs of publication of this article were defrayed in part by the payment of page charges. This article must therefore be hereby marked *advertisement* in accordance with 18 U.S.C. Section 1734 solely to indicate this fact.

[1] Supported in part by Protarga, Inc. (King of Prussia, PA). This work was presented previously in part at the AACR-NCI-European Organization for Research and Treatment of Cancer International Conference on Molecular Targets and Cancer Therapeutics: Discovery, Biology, and Clinical Applications, Miami Beach, Florida, Oct. 29–Nov. 2, 2001.

[2] Present Address: National Cancer Institute, Bethesda, MD 20892.

[3] To whom requests for reprints should be addressed, at Division of Experimental Therapeutics, The Sidney Kimmel Comprehensive Cancer Center at Johns Hopkins, Bunting-Blaustein Cancer Research Building, 1650 Orleans Street, Room 1M87, Baltimore, MD 21231-1000. Phone: (410) 502-7149; Fax: (410) 614-9006; E-mail: sdbaker@jhmi.edu.

[4] The abbreviations used are: CrEL, Cremophor EL; CrEL-P, Cremophor EL-P; DHA, docosahexaenoic acid; HSA, human serum albumin; AAG, α_1-acid glycoprotein; LLOQ, lower limit of quantitation; ULOQ, upper limit of quantitation; EPA, eicosapentaenoic acid; AUC, area under the drug concentration-time curve; ANC, absolute neutrophil count; OFV, objective function value.

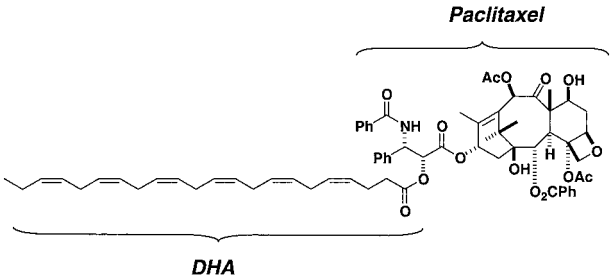

Fig. 1 Chemical structure of DHA-paclitaxel.

paclitaxel at the recommended dose of 1100 mg/m^2 was shown to be very distinct from that of other known taxanes and characterized by an extremely small volume of distribution (~4 liters) and slow systemic clearance (~0.11 liters/h; Ref. 12). Here, we studied the blood distribution of DHA-paclitaxel *in vitro* and *in vivo* in more detail to elucidate the basis for the unique pharmacokinetic behavior of the drug, and additionally investigated the relationship between systemic exposure measures and the dose-limiting toxicity, neutropenia.

MATERIALS AND METHODS

Chemicals and Reagents. Paclitaxel powder (batch, 484034; purity, 98.3%) was kindly provided by Bristol-Myers Squibb (Woerden, the Netherlands). Separate lots of [*G*-^{3}H]-paclitaxel [batch I: specific activity, 8.63 mCi/mg in neat ethanol; batch II: specific activity, 22.9 mCi/mg in toluene-ethanol (98:2)] were provided by Moravek Biochemicals, Inc. (Brea, CA) and Protarga, Inc. (King of Prussia, PA), respectively. Ethanolic reference solutions of DHA-paclitaxel (batch, 710303A; 2.1-ml vials containing 100 mg/ml), [^{3}H]DHA-paclitaxel (specific activity, 116 μCi/mg), CrEL-P reference material (batch, 11255666), EPA-paclitaxel, and cephalomannine were also obtained from Protarga. HSA (fraction V) and AAG (purified from Cohn fraction VI) were from Sigma Chemical (St. Louis, MO). Other chemicals were of reagent grade or better. Human blood was obtained from healthy volunteers, and the plasma fraction was separated by centrifugation (3000 × *g* for 5 min at 37°C) and used within 1 h after collection. Purified water was obtained by filtration and deionization using a Milli-Q-UF system (Millipore, Milford, MA), and was used throughout.

***In Vitro* Binding Experiments.** Equilibrium dialysis was performed at 37°C in a humidified atmosphere of 5% CO_2 using test cells made from 2.0-ml polypropylene Safe-Lock vials (Eppendorf, Hamburg, Germany) carrying a 260-μl inside recess in the lids (13). The experiments were carried out with 260-μl aliquots of either plasma or protein solution (HSA, 40 mg/ml or AAG, 1.0 mg/ml) containing various concentrations of DHA-paclitaxel (0, 1, 10, 100, or 1,000 μg/ml) in the presence of a fixed tracer amount of [^{3}H]DHA-paclitaxel, against an equal volume of PBS. Spectra/Por dialysis tubing with a 12,000–14,000 molecular weight cutoff (Spectrum Medical, Kitchener, Ontario, Canada) was used as dialysis membrane and was soaked for 10 min in a PBS solution before use. Preliminary experiments established that: (*a*) the time to reach equilibrium between plasma proteins and the buffer compartment for DHA-paclitaxel is attained around 20 h, both in the presence and absence of CrEL-P (data not shown); and (*b*) the pH (range, 6.2–7.7) had no influence on DHA-paclitaxel binding characteristics ($P = 0.48$; not shown). Hence, experiments were performed using a 24-h dialysis period at pH 7.4. After this time period, 150-μl aliquots of both compartments were transferred to scintillation vials and mixed with 1.9 ml of Ultima Gold XR scintillation mixture (Packard Bioscience, Groningen, the Netherlands). After vigorous mixing for 30 s, the radiolabel was quantified by liquid-scintillation counting using a Model 1409 counter (Wallac Oy, Turku, Finland) until a preset time of 20 min was reached. With the final method, the mean relative SD in unbound drug fraction of DHA-paclitaxel spiked plasma samples (1, 10, 100, and 1,000 μg/ml) was 15.2%, with values for within-run and between-run precision ranging from 6.88% to 9.86% and 5.23% to 19.1%, respectively.

The effect of CrEL-P and paclitaxel on binding of DHA-paclitaxel was evaluated at final concentrations of 0.25 to 10 μl/ml and 1.0 μg/ml, respectively. Similarly, the influence of DHA-paclitaxel (1–1000 μg/ml) on paclitaxel binding to plasma was evaluated in the presence and absence of CrEL-P.

All of the experiments were performed in triplicate on four separate occasions ($n = 12$), except for the HSA and AAG binding (2 occasions; $n = 6$), and statistical analyses were carried out using NCSS v5.X (J. L. Hintze, Kayesville, UT). The effects of DHA-paclitaxel concentration, CrEL-P, and pH on DHA-paclitaxel binding were estimated by a one-way ANOVA followed by the Dunnett test. The effects of paclitaxel on DHA-paclitaxel binding and *vice versa* was evaluated by a two-tailed unpaired Student's *t* test with equal variances, as recognized by the *F* test.

Estimation of Binding Parameters. The drug concentration ratio in the buffer and plasma or protein solution after dialysis was calculated for each paired observation, and was taken as an estimate of the unbound drug fraction (fu). The bound drug fraction (fbd) was calculated as:

$$\text{fdb} = (1 - \text{fu}) \times 100\% \qquad \text{(A)}$$

Modified Scatchard plots were constructed using the bound drug concentration (Cbd) and the unbound drug concentration (Cu), and initial estimates of binding parameters were obtained using an automated-model selection procedure implemented in the Siphar v4.0 software package (InnaPhase, Philadelphia, PA). The observed data were fitted to the equations for saturable (Eq. B) and nonsaturable binding (Eq. C):

$$\text{Cbd} = \sum_{l=1}^{m} (n_i P \times K_i \times \text{Cu})/(1 + K_i \times \text{Cu}) \qquad \text{(B)}$$

$$Cbd = (nK) \times \text{Cu} \qquad \text{(C)}$$

where Cbd and Cu are expressed as molar concentrations, m is the number of binding site classes, n the number of saturable binding sites per mol of protein in the i-th class (1, 2, or 3), *P* the molar concentration of protein, *K* the association constant, and *nK* the contribution constant of nonspecific, nonsaturable binding on one site. Binding parameters were calculated by an

Table 1 Patient demographic data ($n = 23$)

Characteristic	Median	Range
Baseline screening		
Age (years)	62	29–80
Sex (male/female)[a]	13/10	
BSA (m^2)[b]	1.83	1.36–2.66
Height (cm)	170	155–188
Weight (kg)	75	43–90
Pretherapy hematology		
Hematocrit (%)	39.2	34.6–40.2
Neutrophils ($\times 10^9$/liter)	4.43	2.57–12.1
Platelets ($\times 10^9$/liter)	284	148–589
Pretherapy clinical chemistry		
ASAT (IU/L)	28	14–73
ALAT (IU/L)	19	8.0–41
ALP (IU/L)	103	80–2288
Total bilirubin (mg/dl)	0.5	0.3–1.3
Serum creatinine (mg/dl)	0.80	0.60–1.6
Creatinine clearance (ml/min)	103	31.9–169
Serum albumin (mg/ml)	39	33–53

[a] Data indicate number of patients.
[b] BSA, body-surface area; ASAT, aspartate aminotransferase; ALAT, alanine aminotransferase; ALP, alkaline phosphatase.

iterative nonlinear regression analysis, using the Powell minimization algorithm and weighted least squares with a weight equal to $1/y$. The models were evaluated by the Akaike Information Criterion, weighted sum of squared deviations and the coefficient of variation for each parameter.

Patients and Treatment. Thirteen male and 10 female patients were enrolled into this study; demographic data are presented in Table 1. Trial design, inclusion and exclusion criteria, premedication regimens, and detailed clinical profiles have been documented elsewhere (12). The clinical DHA-paclitaxel preparation (Taxoprexin Injection; Protarga, Inc.) contained 200 mg of the drug formulated in a 5-ml mixture of CrEL-P and dehydrated ethanol (48:52, v/v), and was additionally diluted in 250 ml of 5% (w/v) dextrose in water. Individual drug doses were normalized to body-surface area, and administered once every 3 weeks as a 2-h continuous i.v. infusion (range, 1.83–4.08 h) using an infusion system with in-line 0.22-μm filter at doses ranging from 200 to 1100 mg/m^2. The clinical protocol was approved by the local institutional review board (The Sidney Kimmel Comprehensive Cancer Center at Johns Hopkins), and all of the patients provided written informed consent before entering the study.

Blood Sampling Procedure. Blood samples were collected in Vacutainer tubes from a peripheral site contralateral to the infusion site at the following time points: 10 min before infusion, at the end of infusion, and at 15 and 30 min, 1, 2, 4, 8, and 24 h after the end of infusion. In 12 patients, additional samples were obtained at 15 min after the start of infusion, at 48 and 72 h after the end of infusion, and during the first and second weekly evaluation (approximately days 8 and 15). For subsequent courses, a trough sample was obtained 10 min before drug administration and at the end of infusion. Biological samples were immediately placed in an ice-water bath, centrifuged within 30 min of collection at $1000 \times g$ for 10 min at 4°C, and were stored at or below −70°C until analysis.

Measurement of Total Drug in Plasma. Total drug concentrations of DHA-paclitaxel and paclitaxel in plasma were determined under Good Laboratory Practice at the Kansas City Facility of Applied Analytical Industries International (AAII-KC, Shawnee, KS) by analytical assays based on high-performance liquid chromatography with tandem mass spectrometric detection that were developed and validated by AAII-KC according to the Food and Drug Administration guidelines.[5] Two different methods were used to obtain values for DHA-paclitaxel plasma concentrations. In the first, DHA-paclitaxel concentrations were quantitated in plasma over the range of 5–1,100 μg/ml. A different set of calibration standards was prepared for each Taxoprexin dose level to achieve expected levels of DHA-paclitaxel and CrEL (14) in patient samples according to the following scheme: (*a*) dose level 200 mg/m^2: LLOQ, 5.0 μg/ml; ULOQ, 200 μg/ml; CrEL-P, 640 μg/ml; (*b*) dose level 400 mg/m^2: LLOQ, 10.0 μg/ml; ULOQ, 400 μg/ml; CrEL-P, 1280 μg/ml; (*c*) 660 mg/m^2: LLOQ, 16.5 μg/ml; ULOQ, 660 μg/ml; CrEL-P, 2,112 μg/ml; (*d*) 880 mg/m^2: LLOQ, 22.0 μg/ml; ULOQ, 880 μg/ml; CrEL-P, 2,816 μg/ml; and (*e*) 1,100 mg/m^2: LLOQ, 27.5 μg/ml; ULOQ, 1,100 μg/ml; CrEL-P, 3,520 μg/ml. Samples with values for DHA-paclitaxel that were <LLOQ from the first assay were then analyzed for both DHA-paclitaxel and paclitaxel using a second assay with calibration curve standards over the range of 400–20,000 ng/ml and 10–500 ng/ml, respectively. For the first assay, DHA-paclitaxel and the internal standard (EPA-paclitaxel) were isolated from 50 to 100-μl volumes of plasma using a solvent extraction with acetonitrile and then subjected to chromatography. Separations were achieved on a Hypersil ODS analytical column (5-μm particle size; 10 × 2 mm internal diameter; Keystone Scientific, Inc., Bellefonte, PA), using a nonlinear gradient elution with methanol:10 mM ammonium acetate (pH 5.5; 25:75, v/v; solvent A) and neat acetonitrile (solvent B). The solvent program was set as follows: time 0.01–0.75 min, solvent A:B (35:65); time 1.40–2.50 min, solvent A:B (15:85); time 2.50–2.51 min, solvent A:B (5:95); and time 2.51–2.55 min, solvent A:B (35:65). Quantitation was achieved by monitoring the product ions (*m*/*z* 551.1 for both DHA-paclitaxel and EPA-paclitaxel) of precursor ions at *m*/*z* 1181.6 and *m*/*z* 1155.6 for DHA-paclitaxel and EPA-paclitaxel, respectively.

For the second assay, paclitaxel and the internal standard (cephalomannine) were extracted from 100-μl volumes of plasma using acetonitrile solvent extraction before chromatographic analysis. The following modified solvent program was used: time 0.01–0.80 min, solvent A:B (95:5); time 1.40–1.90 min, solvent A:B (15:85); time 2.50–2.51 min, solvent A:B (5:95); and time 2.51–4.40 min, solvent A:B (95:5). Quantitation was achieved by monitoring the product ions (*m*/*z* 568.8 for paclitaxel, *m*/*z* 550.7 for DHA-paclitaxel, and *m*/*z* 263.6 for cephallomannine) of precursor ions at *m*/*z* 871.4, *m*/*z* 1181.6, and *m*/*z* 832.2 for paclitaxel, DHA-paclitaxel, and cephalomannine, respectively. In all of the cases, the flow rate was set at 0.30 ml/min, and the column effluent was monitored by a Perkin-Elmer-Sciex API *III*+ triple-quadruple mass spectrometer (Woodbridge, Ontario, Canada), using a turbo-ionspray

[5] Internet address: http//www.fda.gov/cvm/guidance/published.htm (May, 2001).

source set at 450°C with data collection in a positive polarity mode.

For both assays, system calibration was accomplished by a weighted ($1/x$) linear-regression analysis (correlation coefficient, ≥ 0.996) of the peak area ratio of analyte to internal standard *versus* the nominal concentration of the analyte. Extraction recovery ranged between 95.8% and 105.0%, and 96.3% and 104.7% for DHA-paclitaxel and paclitaxel, respectively. The values for precision and accuracy, obtained by repeated analysis of quality-control samples spiked with the analytes, ranged between 2.3% and 15.6%, and 86.4% and 114.5%, respectively.

Measurement of DHA-Paclitaxel in Whole Blood. The analytical procedure for DHA-paclitaxel concentrations in whole blood samples was based on reversed-phase high-performance liquid chromatography with UV detection. Briefly, 200-μl aliquots of whole blood were extracted and deproteinized with an equal volume of acetonitrile containing 50 μM of cephalomannine, used as internal standard. Supernatants of the extract (injection volume, 10 μl) were injected directly on an analytical column packed with Curosil-G material (4 μM particle size; 250 × 4.6 mm internal diameter; Phenomenex, Torrance, CA), protected by a Curosil-G Guard Pak (6 μM particle size; 30 × 4.6 mm internal diameter; Phenomenex). The mobile-phase solvents were composed of water:acetonitrile (99:1, v/v; solvent A) and acetonitrile (solvent B), and delivered at a flow rate of 1 ml/min using the following program: time 0.01–5.00 min, solvent A:B (50:50); time 8.0–12.0 min, solvent A:B (10:90); and time 13.0–16.0 min, solvent A:B (50:50). UV detection was performed at a wavelength of 230 nm, with absorbance unit at full scale set at 0.20 from 4 to 10 min, and absorbance unit at full scale set at 2.0 from 10 to 16 min. The retention times for the internal standard and DHA-paclitaxel were ~8.90 and 14.3 min, respectively, with an overall chromatographic run time of 16 min.

Measurement of Unbound Concentrations. The fractions unbound (fu) DHA-paclitaxel and unbound paclitaxel in each individual patient plasma sample were determined using equilibrium dialysis as described previously (13). Biological samples were analyzed for total radioactivity (*i.e.*, [^{3}H]DHA-paclitaxel or [^{3}H]paclitaxel) by liquid-scintillation counting as described above. The unbound drug concentrations (Cu) were calculated from the fraction unbound drug (fu) and the total drug concentration (Cp; *i.e.*, the total of unbound, protein bound and CrEL-P associated), as follows:

$$Cu = fu \times Cp \quad (D)$$

Measurement of CrEL in Plasma. Analysis of CrEL concentrations in plasma was performed using an acetonitrile-*n*-butyl chloride extraction followed by a colorimetric dye-binding microassay with Coomassie Brilliant Blue G-250 (Bio-Rad Laboratories, Munchen, Germany) as described in detail elsewhere (15). The absorption maximum of the dye at 595 nm after binding to CrEL and the simultaneous decrease in absorbance at 450 nm were measured within 4 h against a reagent blank using a Bio-Rad Model 550 automated microplate reader (Hercules, CA).

Pharmacological Analysis. Estimates of pharmacokinetic parameters for unbound DHA-paclitaxel, unbound paclitaxel, and CrEL in plasma were derived from individual concentration-time data sets by noncompartmental analysis using the software package WinNonLin v3.0 (Pharsight Corporation, Mountain View, CA). The peak plasma concentrations and the time to peak were the observed values. The AUC was calculated using the linear trapezoidal method from time zero to the time of the final quantifiable concentration (AUC[tf]). The AUC was also extrapolated to infinity by dividing the last measured concentration by the rate constant of the terminal phase (k), determined by linear-regression analysis. The systemic clearance was calculated by dividing the administered dose by the observed AUC[inf], and the terminal disposition half-life was calculated as ln (2)/k. The systemic exposure to paclitaxel relative to that of DHA-paclitaxel was calculated as:

$$AUC[tf]_{paclitaxel}/AUC[tf]_{DHA\text{-}paclitaxel} \times 100\% \quad (E)$$

after correction for molar differences (molecular weights are 1164 and 854 for DHA-paclitaxel and paclitaxel, respectively). Estimates of pharmacokinetic parameters for total plasma DHA-paclitaxel and paclitaxel were calculated previously (12), and were used to calculate the fraction unbound drug based on the AUC ratio of unbound to total drug (Cu:Cp). The whole blood: plasma concentration ratio (Kb/p) of DHA-paclitaxel was defined as:

$$Kb/p = Cb/Cp \quad (F)$$

The extent of RBC partitioning (Ke/p) was assessed from the relationship:

$$Ke/p = [Kb/p - (1 - Hc)]/Hc \quad (G)$$

with Kb/p depending on hematocrit (Hc) of the whole blood used in the determination. In this relation, pretherapy values of Hc were used from each individual. Representative concentration-time profiles for DHA-paclitaxel in plasma and whole blood, unbound DHA-paclitaxel, and CrEL were fitted with a two-compartment model using the software program MW/Pharm v3.02 (MediWare, Groningen, the Netherlands).

Relationships between exposure to paclitaxel and DHA-paclitaxel (peak concentration or AUC) and hematological toxicity (neutropenia) were explored using nonlinear least squares regression analysis as implemented in Siphar v4.0. Hematological pharmacodynamics were evaluated by analysis of the percentage decrease in ANC, calculated as:

$$\% \text{ decrease} = [(\text{pretherapy value} - \text{nadir value})/\text{pretherapy value}] \times 100\% \quad (H)$$

Data were fitted to a sigmoidal maximum-effect model of drug effect, in which the percentage decrease in ANC (E) is defined as:

$$E = E_0 + E_{max}\,[(KP^{\gamma})/(KP_{50}{}^{\gamma} + KP^{\gamma})] \quad (I)$$

in which E_0 is the no-drug effect, E_{max} is the maximum response (fixed to a value of 100%), KP is the kinetic parameter of interest, KP_{50} is the value of the kinetic parameter predicted to

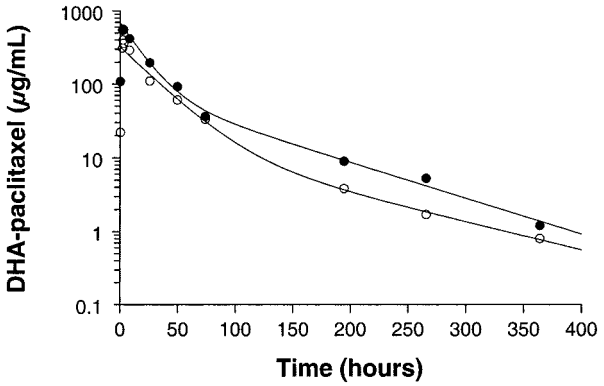

Fig. 2 Representative concentration-time profiles of total DHA-paclitaxel in plasma (*solid symbols*) and whole blood (*open symbols*) in a patient after Taxoprexin administration at a dose of 1100 mg/m^2. Individual curves (*solid lines*) for DHA-paclitaxel concentrations in plasma and whole blood were fitted with a two-compartment model.

result in half of the maximum response, and γ is the Hill constant, describing the sigmoidicity of the curve. Model discrimination was guided by the decrease in the objection function value ($-2\times$ log likelihood), graphical goodness-of-fit analyses, R^2 values, and the Akaike Information Criterion. To differentiate between hierarchical models, $P < 0.05$ was chosen, corresponding to a difference in the OFV of 3.84, with the OFV approximately χ^2 distributed.

Statistical Considerations. All of the data are presented as mean values ± SD, unless stated otherwise, and for all of the tests the *a priori* cutoff for statistical significance was taken at 0.05.

Table 2 Summary of pharmacokinetic parameters[a]

	Dose level (mg/m^2)		
Parameter	660 (6)[b]	880 (5)[b]	1100 (9)[b]
Unbound DHA-paclitaxel			
C_{max} (μg/ml)[c]	1.70 ± 0.72	1.60 ± 0.47	1.88 ± 1.16
tf (h)	26.5 ± 1.9	279 ± 241	325 ± 224
AUC[tf] (μg·h/ml)	17.2 ± 3.6	36.8 ± 23.2	60.2 ± 23.0
AUC[inf] (μg·h/ml)	26.1 ± 10.7	40.3 ± 19.8	62.9 ± 22.1
$T_{1/2,z}$ (h)	17.8 ± 13.4	57.3 ± 45.0	65.8 ± 35.5
CL (liter/h)	58.2 ± 25.3	55.5 ± 32.9	39.2 ± 15.4
Cu/Cp (%)	0.33 ± 0.071	0.25 ± 0.06	0.27 ± 0.13
Unbound paclitaxel			
C_{max} (μg/ml)	0.013 ± 0.011	0.013 ± 0.005	0.021 ± 0.010
tf (h)	26.5 ± 1.9	53.8 ± 25.6	136 ± 87.7
T_{max} (h)	2.14 ± 0.17	2.07 ± 0.32	2.08 ± 0.29
AUC[tf] (μg·h/ml)	0.089 ± 0.029	0.222 ± 0.122	0.624 ± 0.216
AUC[inf] (μg·h/ml)	0.225 ± 0.083	0.353 ± 0.094	0.921 ± 0.414
$T_{1/2,z}$ (h)	40.7 ± 22.4	33.2 ± 5.66	80.7 ± 71.2
Cu/Cp (%)	9.7 ± 0.90	8.3 ± 2.9	7.7 ± 1.5
$AUC[tf]_{pac}/AUC[tf]_{DHA}$ (%)	0.71 ± 0.15	0.91 ± 0.25	1.62 ± 0.88
CrEL			
C_{max} (μl/ml)	2.45 ± 0.41	4.12 ± 0.99	4.86 ± 0.75
tf (h)	23.5 ± 7.5	45.6 ± 27.8	71.0 ± 8.2
AUC[tf] (μl·h/ml)	31.7 ± 12.6	70.7 ± 42.5	120 ± 30.2
AUC[inf] (μl·h/ml)	55.2 ± 18.7	108 ± 56.1	162 ± 53.0
$T_{1/2,z}$ (h)	21.8 ± 4.72	35.9 ± 8.01	36.4 ± 10.7
CL (ml/h)	418 ± 95.9	301 ± 177	238 ± 91.2

[a] Mean values ± SD.
[b] Total number of patients studied at each dose level in parenthesis.
[c] C_{max}, peak plasma concentration; tf, final quantifiable concentration; T_{max}, time to peak plasma concentration; AUC, area under the plasma concentration-time curve; inf, infinity; $T_{1/2,z}$, half-life of the terminal disposition phase; CL, apparent clearance; Cu/Cp, fraction unbound drug based on the AUC ratio of unbound to total drug; pac, paclitaxel; DHA, DHA-paclitaxel.

RESULTS

***In Vitro* Binding Interactions.** In the absence of CrEL-P, DHA-paclitaxel was found to bind extensively (99.6 ± 0.057%) to human plasma proteins, with a free drug fraction of only 0.0038 ± 0.00057. At clinically relevant concentrations of DHA-paclitaxel (1–1000 μg/ml), this binding was concentration independent ($P = 0.63$), indicating a nonspecific, nonsaturable process. In contrast to previous observations with paclitaxel (16), CrEL-P had only a very minor effect on DHA-paclitaxel binding, which was only observed at the two highest CrEL-P concentrations tested ($P < 0.0001$). The free-drug fraction of DHA-paclitaxel was similar in the absence and presence of paclitaxel ($P = 0.19$). DHA-paclitaxel binding to normal physiological levels of HSA (99.8 ± 0.051%) and AAG (99.8 ± 0.037%) was similar to that in plasma, drug-concentration independent ($P > 0.13$), and not influenced by CrEL-P ($P > 0.89$). Regression modeling revealed that the binding to HSA and AAG was nonsaturable on a single site in the concentration range studied, with the bound concentration linearly related to unbound drug ($R^2 > 0.999$; $P = 0.0056$). Binding affinity to both proteins was identical with an association constant for nonsaturable binding (nK) to HSA and AAG of 678 ± 22.5 μM^{-1}.

In the presence of DHA-paclitaxel, the unbound fraction of paclitaxel increased from 0.052 ± 0.0018 to 0.055 ± 0.0036 (relative increase, 6.25%; $P = 0.011$) as the DHA-paclitaxel concentration increased from 0 to 1000 μg/ml, suggesting weakly competitive displacement from protein-binding sites. This effect was not observed in the absence of CrEL-P ($P = 0.65$), with unbound paclitaxel fractions of 0.124 ± 0.0071 (DHA-paclitaxel concentration, 0 μg/ml) and 0.129 ± 0.0079 (DHA-paclitaxel concentration, 1000 μg/ml).

***In Vivo* Blood Distribution.** Concentration-time profiles of DHA-paclitaxel in whole blood followed the same general pattern as those in plasma (Fig. 2). At Taxoprexin doses of 880 mg/m^2 ($n = 2$) and 1100 mg/m^2 ($n = 6$), the DHA-paclitaxel blood:plasma concentration ratios were 0.486 ± 0.202 and 0.536 ± 0.152, respectively. This suggests that the majority of DHA-paclitaxel was associated with the plasma fraction, with a negligible degree of RBC partitioning (Ke/p = −0.113 ± 0.305; $P < 0.05$ *versus* Ke/$P = 0$).

Plasma Pharmacokinetics. Plasma pharmacokinetic parameters at the three highest dose levels are presented in Table 2. Drug concentrations in plasma from patients treated at the two lowest dose levels (200 mg/m^2, $n = 1$; 400 mg/m^2, $n = 2$) remained undetectable beyond 4 h after the end of infusion; pharmacokinetic parameters for these patients are not listed in Table 2. Representative plasma concentration-time profiles for unbound DHA-paclitaxel and paclitaxel are shown in Fig. 3. Moderate interindividual variability in unbound DHA-paclitaxel and paclitaxel AUC was noted at the 1100 mg/m^2 dose level

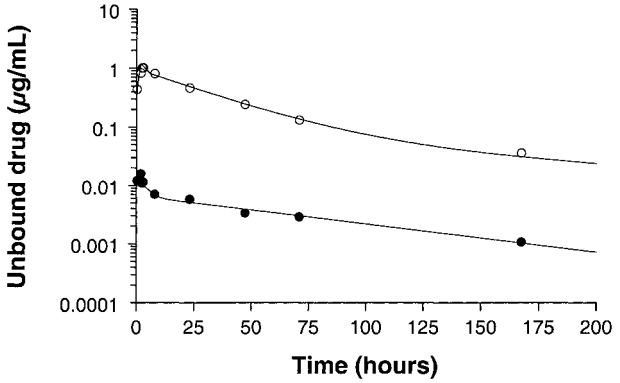

Fig. 3 Representative concentration-time profiles of unbound DHA-paclitaxel (*open symbols*) and paclitaxel (*closed symbols*) in a patient after Taxoprexin administration at a dose of 1100 mg/m^2. Individual curves (*solid lines*) for unbound DHA-paclitaxel and paclitaxel concentrations in plasma were fitted with a two-compartment model.

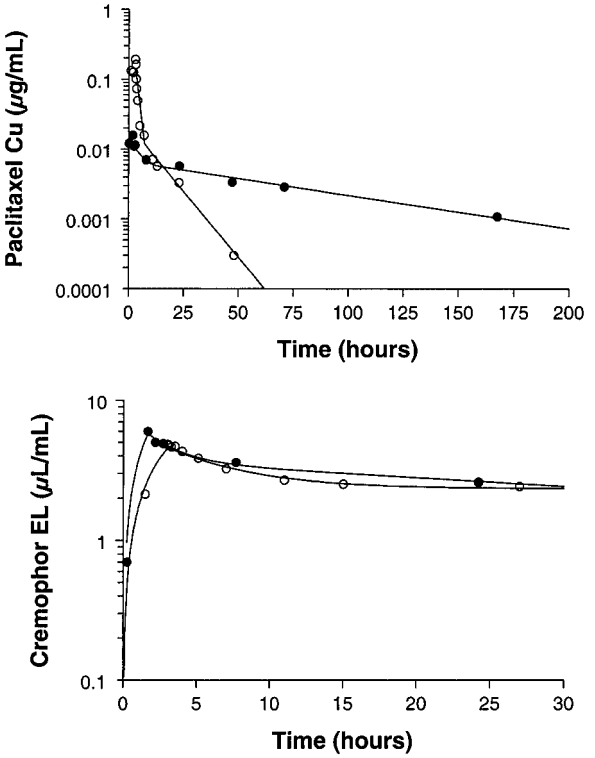

Fig. 4 Representative concentration-time profiles of unbound paclitaxel (*top*) and Cremophor EL (*bottom*) after Taxoprexin administration at a dose of 1100 mg/m^2 (*closed symbols*) or Taxol at a dose of 175 mg/m^2 (*open symbols*; data from Ref. 22). Individual curves (*solid lines*) for unbound paclitaxel and CrEL concentrations after administration of Taxoprexin or Taxol were fitted with a two-compartment model.

(*i.e.*, ~35%). Exposure to unbound DHA-paclitaxel increased in near proportional manner with dose (Table 2), and clearance values were not significantly different between the various dose levels ($P = 0.352$, Kruskal-Wallis test), suggesting a linear and dose-independent pharmacokinetic behavior. Consistent with the *in vitro* data, >99.7% of drug was bound within the circulation without any trend in time (data not shown).

In vivo formation of paclitaxel was rapid (at 15 min during the infusion), with peak concentrations observed around the end of infusion (Table 2; Figs. 3 and 4). However, at the 1100 mg/m^2 dose level, unbound paclitaxel represented only <2% of unbound DHA-paclitaxel exposure. The exposure to unbound paclitaxel increased in a distinct nonlinear fashion with Taxoprexin dose, as a 25% dose increment (from 880 to 1100 mg/m^2) was associated with 70% and 181% increases in peak concentration and AUC[tf], respectively. As a result, systemic exposure to unbound paclitaxel relative to that of unbound DHA-paclitaxel was highly dose-dependent (Table 2), confirming the nonlinear binding process of paclitaxel observed *in vitro*.

CrEL Pharmacokinetics. Disappearance of CrEL from the plasma compartment was characterized by elimination in an apparent biexponential manner (Fig. 4), in line with previous findings (13). A dose dependence was evident in CrEL clearance ($P = 0.049$, Kruskal-Wallis and Dunn's tests; Table 2), which likely relates to inaccurate determination of the terminal disposition phase at the lower Taxoprexin dose levels resulting from constraints in assay sensitivity and the sampling scheme.

Exposure-Toxicity Relationships. The parameter estimates for the different pharmacodynamic models, using data from all 23 of the patients, are summarized in Table 3. Preliminary results demonstrated that separate estimation of the observed maximum effect did not improve the fits, and it was set to a theoretical maximum value of 100%. The kinetic parameters predicted to result in half of the maximum response showed a substantial degree of interindividual variability (range, 24–73%) and were poorly estimated in some models because of the few patients. With the use of peak concentration as exposure measure, the fits were significantly worse than those based on AUC for each individual analyte (ΔOFV ≥9.34; Fig. 5). The exposure-neutropenia relationship was best described with the model based on unbound paclitaxel AUC, although no significant improvement of the fit was obtained as compared with total paclitaxel AUC (ΔOFV = 1.48; Table 3).

DISCUSSION

In the present study we have described the *in vitro* and *in vivo* blood distribution of DHA-paclitaxel, a conjugate of the natural fatty acid DHA and paclitaxel. The binding of DHA-paclitaxel to human plasma was >99.6% and independent of drug concentration over the full clinically relevant range. When binding studies were extended to individual proteins, it was found that HSA and AAG contributed to about an equal extent to drug binding, with an association constant for nonspecific, nonsaturable binding of 678 μM^{-1}. This degree of binding is substantially different from that of paclitaxel, which is 85–87% bound (17), with overall association constants of 1.7 and 0.082 μM^{-1} for specific and nonspecific binding to HSA (18, 19). The presence of the long-chain fatty acid linked to the paclitaxel molecule is the likely explanation for this difference, as fatty acids are among the most strongly protein-bound endogenous substrates (association constant ~100 μM^{-1}; Ref. 20). The binding to proteins also had a dramatic influence on drug distribution to RBCs, in line with the small distribution volume

Table 3 Summary of pharmacodynamic modeling[a]

	Paclitaxel				DHA-paclitaxel			
	Unbound		Total drug		Unbound		Total drug	
Parameter	C_{max}[a]	AUC	C_{max}	AUC	C_{max}	AUC	C_{max}	AUC
KP_{50}	0.003 ± 0.001	0.031 ± 0.007	0.044 ± 0.032	0.300 ± 0.215	0.49 ± 0.31	8.61 ± 2.56	190 ± 55	2616 ± 1040
γ	1.00 ± 0.40	0.77 ± 0.14	1.09 ± 0.44	0.72 ± 0.17	1.10 ± 0.77	1.27 ± 0.39	1.62 ± 0.34	1.10 ± 0.23
E_0	0.0001	0.0001	0.036	0.036	0.0004	0.0001	0.0001	0.0001
OFV	119.8	65.56	95.38	67.04	135.5	79.06	77.42	68.08
AIC	103.4	95.96	101.6	97.33	97.91	95.73	98.96	97.53
R^2	0.253	0.624	0.465	0.602	0.111	0.548	0.530	0.595
P	0.009	<0.0001	0.0006	0.0001	0.14	0.0002	0.0002	0.0001

[a] Mean values (±SD for KP_{50} and γ) from 23 patients using sigmoidal maximum-effect models of exposure-neutropenia relationships.
[b] C_{max}, peak plasma concentration; AUC, area under the plasma concentration-time curve; KP_{50}, kinetic parameter predicted to result in half of the maximum response expressed in units of μg/mL for C_{max} and in units of μg · h/mL for AUC; γ, Hill constant; E_0, no-drug effect; AIC, Akaike Information Criterion.

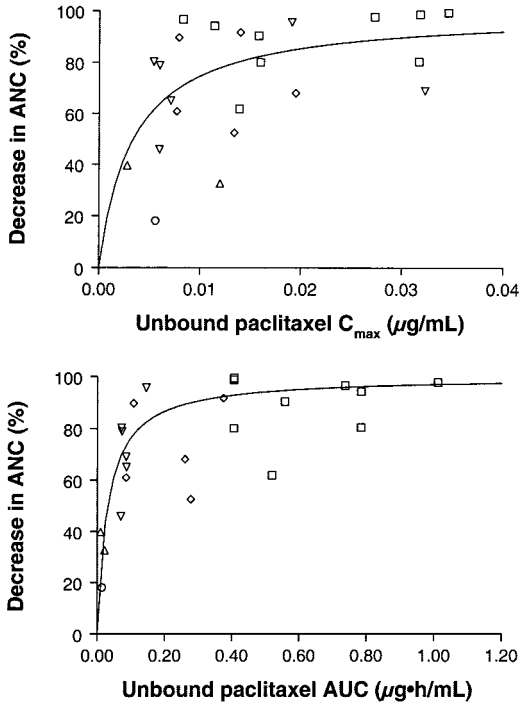

Fig. 5 Percentage decrease in ANC as a function of peak concentration (C_{max}) of unbound paclitaxel (*top*) and AUC of unbound paclitaxel (*bottom*) in 23 patients treated with Taxoprexin DHA-paclitaxel at doses ranging from 200 to 1100 mg/m^2 (○, 200 mg/m^2; △, 400 mg/m^2; ▽, 660 mg/m^2; ◇, 880 mg/m^2; and □, 1100 mg/m^2). The *solid lines* represent the fit of a sigmoidal maximum-effect model to the data.

of DHA-paclitaxel and previous studies of other drugs demonstrating that RBC partitioning only involves the unbound fraction (21).

It has been shown that CrEL has a major impact on paclitaxel binding (16). Although the mechanism underlying this interaction has not yet been fully elucidated, the presence of CrEL in solution as large polar micelles is thought to entrap paclitaxel. In contrast, a decreased fraction of unbound DHA-paclitaxel *in vitro* was only observed at CrEL levels measurable at the highest dose tested clinically (~5 μl/ml). This is consistent with the dose-dependent peak concentrations of DHA-paclitaxel observed here as well as in tumor-bearing mice, wherein peak levels reached values of 29 and 61 μM at doses of 27.4 and 120 mg/kg, respectively (11). Typical for slow clearance drugs, this phenomenon did not significantly influence overall disposition profiles, and a linear pharmacokinetic behavior for unbound DHA-paclitaxel was found in the tested dose range of 200-1100 mg/m^2.

Across all of the dose levels, paclitaxel declined in parallel with DHA-paclitaxel, suggesting that the elimination rate constant of the prodrug is smaller than that of the metabolite and that paclitaxel elimination is formation-rate limited. This is consistent with the ~15-fold difference in apparent half-life of unbound paclitaxel after Taxoprexin Injection (*i.e.*, 80.7 ± 71.2 h) and Taxol administration (6.12 ± 3.42 h; Ref. 22). At the recommended doses, 10-fold lower peak concentrations of unbound paclitaxel were achieved with Taxoprexin administration (1100 mg/m^2) as compared with Taxol (175 mg/m^2; 0.021 ± 0.010 *versus* 0.197 ± 0.099 μg/ml), whereas the AUC values were very similar (0.624 ± 0.216 *versus* 0.526 ± 0.099 μg•h/ml; Ref. 22).

The present study demonstrates a striking dose dependence in unbound paclitaxel pharmacokinetics after Taxoprexin administration, with the peak concentration and AUC increasing >2-fold with a 1.25-fold increase in dose (from 880 to 1100 mg/m^2). There are many drugs that display nonlinear elimination kinetics, most commonly resulting from saturable metabolic pathways (*e.g.*, phenytoin; Ref. 23) or saturable excretion pathways (*e.g.*, cyclophosphamide; Ref. 24). However, it is very unlikely that this also accounts for the nonlinear exposure to paclitaxel, because: (*a*) the apparent Michaelis-Menten constants for the principal metabolic route (*i.e.*, paclitaxel 6α-hydroxylation) for human hepatic microsomes (~4.0 μM) and complementary expressed CYP2C8 (~5.4 μM) are >160-fold higher than concentrations of unbound paclitaxel in patients (25); and (*b*) no signs of nonlinearity in paclitaxel tissue distribution and fecal or urinary excretion have been noted after administration of Taxol (26, 27). Although the mechanistic basis for the dose-dependent pharmacokinetics of paclitaxel observed here remains to be elucidated, it is possible that capacity-limited

binding to plasma proteins in the presence of DHA-paclitaxel contributes to explaining this phenomenon. Support for this hypothesis comes from *in vitro* studies indicating that paclitaxel binding is slightly altered by clinically relevant concentrations of DHA-paclitaxel as a result of a displacement interaction. Some clinical implications from this process, particularly with respect to considerations of treatment schedule, are easily envisaged. Most importantly, it makes the use of total paclitaxel concentrations for therapeutic monitoring misleading, particularly if there is significant interindividual variability in the apparent binding constant. In addition, changes in proteins levels, which are known to occur in cancer patients, can result in time dependence of drug kinetics, especially with respect to total drug (28).

The pharmacodynamic analysis performed here, based on nonlinear sigmoidal maximum-effect models, revealed significant correlations between the percentage decrease in ANC at nadir and exposure to paclitaxel. The predicted AUC value of unbound paclitaxel associated with a 50% decrease in ANC (KP_{50}) was only 0.031 μg·h/ml after Taxoprexin administration and ~0.790 μg·h/ml after Taxol in a 3 weekly regimen (17), despite similar sigmoidicity factors and exposure levels. Although DHA-paclitaxel has no microtubule-assembly activity *in vitro* and is thought to be inactive until metabolized (11), the present results showed a significant relationship between DHA-paclitaxel exposure and neutropenia. This suggests that the extended exposure of bone marrow cells to high levels of DHA-paclitaxel as a result of the small distribution volume can result in localized toxicity and contribute to the kinetic-dynamic relationships. The present data did not support, possibly because of insufficient information, the notion that the unbound concentration should be more closely related to drug effects than total concentrations. To additionally optimize kinetic-dynamic relationships, a population analysis for Taxoprexin-induced myelosuppression is being performed currently by modeling the entire time course of neutrophils in each individual patient.[6]

Previous studies have shown that CrEL clearance increases with prolonged duration of infusion from 1 to 3 and 24-h, and that systemic exposure to CrEL depends significantly on the duration of drug infusion (29). Our current data on CrEL levels in patients treated with Taxoprexin Injection given as a 2-h infusion, can therefore not be compared directly with other infusion schedules. However, it is noteworthy that the mean CrEL clearance of 302 ± 133 ml/h observed here is consistent with previous estimates of 199 ± 70.0 ml/h and 361 ± 175 ml/h after 1-h and 3-h administrations of Taxol, respectively (30). This provides additional evidence of the time dependence in CrEL clearance, with disproportional increases in systemic exposure being associated with shortening of infusion duration. This finding may be of particular importance in view of the potential role of CrEL in the etiology of acute hypersensitivity reactions associated with its clinical use. Szebeni *et al.* (31) have postulated that an important contributing mechanism to these hypersensitivity reactions is related to complement activation because of binding of natural anticholesterol antibodies to the hydroxyl-rich surface of CrEL micelles. Although only few episodes of minor acute reactions were observed in the Phase I study of Taxoprexin Injection (mainly facial flushing graded 1 on the National Cancer Institute common toxicity scale; 2 patients in cycle 1 and another 5 beyond cycle 1),[7] it should be mentioned that a change in Taxoprexin Infusion duration can have a much greater impact on complement-activating CrEL levels at the site of administration and on total CrEL exposure than would be expected in case of time-independent pharmacokinetics.

It is concluded that DHA-paclitaxel binding to plasma proteins is an important determinant of its pharmacokinetic behavior. The major fraction of the administered drug is sequestered by HSA and AAG, restricting the unbound concentration, and affecting distribution and elimination pathways. A comparative analysis indicates that exposure to CrEL and unbound paclitaxel after Taxoprexin administration at the recommended dose is similar to that achieved with Taxol on clinically relevant schedules.

Additional analysis of the disposition of DHA-paclitaxel in patients, with respect to the current findings, should be of great importance for our ability to better understand the role of the various factors that may influence the pharmacologic behavior and actions of the drug, and of other drugs administered concomitantly.

REFERENCES

1. Adams, J. D., Flora, K. P., Goldspiel, B. R., Wilson, J. W., Arbuck, S. G., and Finley, R. Taxol: a history of pharmaceutical development and current pharmaceutical concerns. J. Natl. Cancer Inst. Monogr., *15:* 141–147, 1993.

2. Nuijen, B., Bouma, M., Schellens, J. H., and Beijnen, J. H. Progress in the development of alternative pharmaceutical formulations of taxanes. Investig. New Drugs, *19:* 143–153, 2001.

3. Gueritte, F. General and recent aspects of the chemistry and structure-activity relationships of taxoids. Curr. Pharm. Des., *7:* 1229–1249, 2001.

4. Huang, P. S., and Oliff, A. Drug-targeting strategies in cancer therapy. Curr. Opin. Genet. Dev., *11:* 104–110, 2001.

5. Rodrigues, M. L., Carter, P., Wirth, C., Mullins, S., Lee, A., and Blackburn, B. K., Synthesis and β-lactamase-mediated activation of a cephalosporin-Taxol prodrug. Chem. Biol., *2:* 223–227, 1995.

6. de Groot, F. M., van Berkom, L. W., and Scheeren, H. W. Synthesis and biological evaluation of 2′-carbamate-linked and 2′-carbonate-linked prodrugs of paclitaxel: selective activation by the tumor-associated protease plasmin. J. Med. Chem., *43:* 3093–3102, 2000.

7. Damen, E. W., Nevalainen, T. J., van den Bergh, T. J., de Groot, F. M., and Scheeren, H. W. Synthesis of novel paclitaxel prodrugs designed for bioreductive activation in hypoxic tumour tissue. Bioorg. Med. Chem., *10:* 71–77, 2002.

8. Safavy, A., Raisch, K. P., Khalzaeli, M. B., Buchsbaum, D. J., and Bonner, J. A. Paclitaxel derivatives for targeted therapy of cancer:

[6] R. Xie, S. D. Baker, A. Sparreboom, C. V. R. Black, and M. O. Karlsson. Semi-mechanistic model for hematological toxicities of DHA-paclitaxel, manuscript in preparation.

[7] A. C., Wolff, R. C. Donehower, M. K. Carducci, M. A. Carducci, J. R. Brahmer, Y. Zabelina, M. O. Bradley, F. H. Anthony, C. S. Swindell, P. A. Witman, N. L. Webb, and S. D. Baker. Phase I study of DHA-paclitaxel: a taxane-fatty acid conjugate with a unique pharmacology and toxicity profile, submitted for publication.

toward the development of smart taxanes. J. Med. Chem., *42:* 4919–4924, 1999.

9. Luo, Y., Ziebell, M. R., and Prestwich, G. D. A hyaluronic acid-Taxol antitumor bioconjugate targeted to cancer cells. Biomacromolecules, *1:* 208–218, 2000.

10. Sauer, L. A., Dauchy, R. T., and Blask, D. E. Mechanism for the antitumor and anticachectic effects of *n*-3 fatty acids. Cancer Res., *60:* 5289–5295, 2000.

11. Bradley, M. O., Webb, N. L., Anthony, F. H., Devanesan, P., Witman, P. A., Hemamalini, S., Chander, M. C., Baker, S. D., He, L., Horwitz, S. B., and Swindell, C. S. Tumor targeting by covalent conjugation of a natural fatty acid to paclitaxel. Clin. Cancer Res., *7:* 3229–3238, 2001.

12. Wolff, A. C., Baker, S. D., Bowling, M. K., Carducci, M. A., Bradley, M. O., Anthony, F. H., Swindell, C. S., Witman, P. A., Webb, N. L., and Donehower, R. C. Phase I study of *Taxoprexin*® DHA-paclitaxel (Txp), a novel taxane with unique preclinical activity, pharmacology, and toxicity profile. Proc. Am. Soc. Clin. Oncol., *19*: 921E, 2000.

13. Brouwer, E., Verweij, J., de Bruijn, P., Loos, W. J., Pillay, M., Buijs, D., and Sparreboom, A. Measurement of fraction unbound paclitaxel in human plasma. Drug Metab. Dispos., *28:* 1141–1145, 2000.

14. Sparreboom, A., Verweij, J., van der Burg, M. E. L., Loos, W. J., Brouwer, E., Vigano, L., Locatelli, A., de Vos, A. I., Nooter, K., Stoter, G., and Gianni, L. Disposition of Cremophor EL in humans limits the potential for modulation of the multidrug resistance phenotype *in vivo*. Clin. Cancer Res., *4:* 1937–1942, 1998.

15. Brouwer, E., Verweij, J., Hauns, B., Loos, W. J., Nooter, K., Mross, K., Stoter, G., and Sparreboom, A. Linearized colorimetric assay for Cremophor EL: application to pharmacokinetics after 1-hour paclitaxel infusions. Anal. Biochem., *261:* 191–202, 1998.

16. Sparreboom, A., van Zuylen, L., Brouwer, E., Loos, W. J., de Bruijn, P., Gelderblom, H., Pillay, M., Nooter, K., Stoter, G., and Verweij, J. Cremophor EL-mediated alteration of paclitaxel distribution in human blood: clinical pharmacokinetic implications. Cancer Res., *59:* 1454–1457, 1999.

17. Henningsson, A., Karlsson, M. O., Vigano, L., Gianni, L., Verweij, J., and Sparreboom, A. Mechanism-based pharmacokinetic model for paclitaxel. J. Clin. Oncol., *19:* 4065–4073, 2001.

18. Purcell, M., Neault, J. F., and Tajmir-Riahi, H. A., Interaction of Taxol with human serum albumin. Biochim. Biophys. Acta, *1478:* 61–68, 2000.

19. Paál, K., Müller, J., and Hegedûs, L. High affinity binding of paclitaxel to human serum albumin. Eur. J. Biochem., *268:* 2187–2191, 2001.

20. Bhattacharya, A. A., Grune, T., and Curry, S. Crystallographic analysis reveals common modes of binding of medium and long-chain fatty acids to human serum albumin. J. Mol. Biol., *303:* 721–732, 2000.

21. Hinderling, P. Red blood cells: a neglected compartment in pharmacokinetics and pharmacodynamics. Pharmacol. Rev., *49:* 279–295, 1997.

22. Sparreboom A., Spicer D., Verweij J., Loos W. J., Doroshow J. D., and Synold T. W. Effect of valspodar (PSC 833) on the pharmacokinetics of unbound paclitaxel. Proc. Am. Assoc. Cancer Res., *42:* 535–536, 2001.

23. Bauer, L. A., and Blouin, R. A. Phenytoin Michaelis-Menten pharmacokinetics in Caucasian paediatric patients. Clin. Pharmacokinet., *8:* 545–549, 1983.

24. Chen, T. L., Passos-Coelho, J. L., Noe, D. A., Kennedy, J., Black, K. C., Colvin, O. M., and Grochow, L. B. Nonlinear pharmacokinetics of cyclophosphamide in patients with metastatic breast cancer receiving high-dose chemotherapy followed by autologous bone marrow transplantation. Cancer Res., *55:* 810–816, 1995.

25. Rahman, A., Korzekwa, K. R., Grogan, J., Gonzalez, F. J., and Harris, J. W. Selective biotransformation of Taxol to 6α-hydroxytaxol by human cytochrome P450 2C8. Cancer Res., *54:* 5543–5546, 1994.

26. Sparreboom, A., van Tellingen, O., Nooijen, W. J., and Beijnen, J. H. Nonlinear pharmacokinetics of paclitaxel in mice results from the pharmaceutical vehicle Cremophor EL. Cancer Res., *56:* 2112–2115, 1996.

27. van Zuylen, L., Karlsson, M. O., Verweij, J., Brouwer, E., de Bruijn, P., Nooter, K., Stoter, G., and Sparreboom, A. Pharmacokinetic modelling of paclitaxel encapsulation in Cremophor EL micelles. Cancer Chemother. Pharmacol., *47:* 309–318, 2001.

28. Ludden, T. M. Nonlinear pharmacokinetics. Clin. Pharmacokinet., *20:* 429–446, 1991.

29. van Zuylen, L., Gianni, L., Verweij, J., Mross, K., Brouwer, E., Loos, W. J., and Sparreboom, A. Inter-relationships of paclitaxel disposition, infusion duration and cremophor EL kinetics in cancer patients. Anticancer Drugs, *11:* 331–337, 2000.

30. Gelderblom, H., Mross, K., ten Tije, A. J., Behringer, D., Mielke, S., van Zomeren, D. M., Verweij, J., and Sparreboom, A. Comparative pharmacokinetics of unbound paclitaxel during 1- and 3-hour infusions. J. Clin. Oncol., *20:* 574–581, 2002.

31. Szebeni, J., Muggia, F. M., and Alving, C. R. Complement activation by Cremophor EL as a possible contributor to hypersensitivity to paclitaxel: an *in vitro* study. J. Natl. Cancer Inst. (Bethesda), *90:* 300–306, 1998.